Available online at www.sciencedirect.com

ScienceDirect

Energy Procedia 51 (2014) 334 – 343

Energy Procedia

7th Trondheim CCS Conference, TCCS-7, June 5-6 2013, Trondheim, Norway

Large-scale numerical modelling of CO_2 injection and containment phases for an Italian near-coast reservoir using PFLOTRAN

Paolo Orsini[a], Barbara Cantucci[b], Fedora Quattrocchi[b]

[a]*BLOSint LTD, Triumph Road , Nottingham, NG7 2TU, UK*
[b]*Istituto nazionale di geofisica e vulcanologia, Via Vigna murata 605, 00141 Roma, Italy*

Abstract

A potential CO_2 storage site located offshore the west coast of Italy, has been modelled using PFLOTRAN assuming an injection rate of 1.5 Mtons/year for 20 years. The model predicts a CO_2 footprint characterised by a diameter of about 3.5 km and a maximum pressure build up of 38 bars. The solubility trapping has been quantified, predicting a dissolution in brine of 69% and 79% of the total amount of CO_2 injected after 1000 and 2000 years respectively. The residual trapping has also been found to play an important role, with 9% and 6% of the injected CO_2 being locked into the hosting matrix pores after 1000 and 2000 years respectively. Considering a worst-case scenario for leakages, where zero critical capillarity pressure has been assumed, minor CO_2 leakages through the caprock have been identified, caused by the combined effects of the long-term structural trapping and the large and lasting overpressure caused by the CO_2 injection in an ideally closed system. Finally, some preliminary work undertaken as part of an ongoing effort to couple a geochemical model to the multi-phase flow simulations reveals i) small changes in mineral volume fraction and porosity during and after the injection (~5% after 1000 years), and ii) a not negligible self-sealing effect due to precipitation of calcite in the lower layer of the caprock. Further investigations and longer physical time runs are needed to confirm this assumption, but also to gain more confidence on the geochemical model built so far and to estimate the mineral trapping potential for this site.

Selection and peer-review under responsibility of SINTEF Energi AS

Keywords: CO2 geological storage modelling; geochemistry; PFLOTRAN; PFLOTRAN case study;

1. Introduction

Carbon geological storage (CGS) in deep saline aquifers is considered one of the most promising technologies to reduce anthropogenic CO_2 emissions into the atmosphere, which are blamed by a large part of the scientific community as one of the main causes of current climate change. Due to the large space and time scale involved in the CGS, numerical models are essential tools in predicting the long-term behaviour of the CO_2 injected

Selection and peer-review under responsibility of SINTEF Energi AS
doi:10.1016/j.egypro.2014.07.040

underground. However, the physical phenomena involved are rather complex, and their different nature requires a multi-disciplinary approach. Thermal effects, hydrogeology, geochemistry and geomechanics need to be considered simultaneously in order to build realistic numerical models able to predict the CO_2 long-term fate and the reservoir response during the injection and containment phases. Consequently, the numerical solutions for these types of problems are computationally demanding, and the use of parallel software becomes essential to produce predictions in a relatively short time. In this work, a large-scale model of an Italian site, studied as a potential candidate for CO_2 storage, was built using PFLOTRAN, a sub-surface reactive flow software with parallel capabilities [1]. The study is an example of the use of parallel software to assess CO_2 solubility and mineral trapping that are expected to occur in much longer times than structural trapping, requiring numerical solutions that cover physical times of thousands of years. The main aim is to analyse the long-term fate of the injected CO_2 for the specific site considered, including solubility and trapping mechanisms. Particular attention is given to the reservoir-caprock interface, and the minerals' reaction processes to assess its sealing capacity.

2. Potential CO_2 storage site and geological model construction

The site considered in this CGS feasibility study is a carbonate reservoir, located off-shore in the Tyrrhenian sea within an isolated horst structure surrounded by caprock units. The normal faults (presently inactive), which delimit horizontally the reservoir, have been considered impermeable. They have not been included in the model, however, to take account of their vicinity and to consider the overpressure worst-case scenario during the CO_2 injection, no-flux conditions have been imposed to the vertical domain boundaries.

The stratigraphy is constrained by a deep well that evidences a thick succession consisting of, from the top to the bottom, Plio-Quaternary marine units unconformably deposited on a Cretaceous-Oligocene flyshoid succession (both considered efficient caprock). They are superimposed on a Jurassic-Cretaceous, mainly calcareous, succession, (which hosts a regional aquifer) and Upper Triassic evaporates, Fig. 1.a. The reservoir extends downwards from a minimum depth of ~1600 m to ~4000 m below sea level (b.s.l).

A 3D geological model was built combining the stratigraphical data and seismic reflection lines, Fig. 1.b, 1.c. The conceptual model covers an area of 13.5 x 12.75 km and a vertical development of more than 3 km, from the sea bottom to the basement of the structure.

3. Computational model

The salinity of the deep formation waters (24 g/L) has been measured during the drilling of the well, while the petrophysical properties of the aquifer-hosting rock and of the sealing layers (Table 1) have been computed using the mineralogical composition, the thermal properties of rocks and by heat flux analysis, [2]. Bulk mineralogical composition was obtained by analysing the inland outcropping samples representative of the 11 zones according to the log data. Only 9 of the 11 zones shown in the log data have been considered in this work, cutting a portion of the caprock to reduce the computational domain and consequently the computational cost. Two hypotheses have been considered: a reduced caprock made only of layer 4 and 5, and a larger caprock portion including also ~300 m of layer 3, see Fig 1.a. Unless stated otherwise, the thinner caprock is used in the simulations. The effect of cutting a portion of the caprock has been assessed in section 3.1.

The first four layers from the top have a very low permeability ($\sim 10^{-17}$ m^2) and are part of the caprock. The underlying four layers, extending from a minimum depth of 1600 m to a maximum of about 4000 m, have a higher permeability ($\sim 10^{-14}$ m^2) and represent the target reservoir. Finally, at the bottom, a strata characterised by a very low permeability ($\sim 10^{-16}$ m^2) acts as the lower confining layer. Each layer is assumed to have homogeneous and isotropic properties, Table 1.

The horizontal extension of the model is 13.5 x 12.75 km, and since the purpose of the model is to analyse the long-term fate of the CO_2, the injection well, located in the upper part of the reservoir at a depth of ~1970 m,

approximately in the middle of the domain (x=7125 m, y=6125 m), is modelled with a source inside an injection cell that has the following dimensions: 250 x 250 x 30 m, Fig. 1.c. An injection of 1.5 Mtons/year of CO_2 is considered for a period of 20 years. Due to the depth of the reservoir, only supercritical (SC) CO_2 is expected. The domain is discretised with a hexahedron-cell mesh that follows the geological layers: the horizontal resolution in x and y is equal to 250 m, and the vertical resolution goes from a minimum of 30 m in the injection and caprock regions, to a maximum of 300 m, Fig. 2. Even if the thicker cells are deployed away from the CO_2 plume, this is a coarse mesh, which can introduce a not negligible numerical diffusion, hence leading to an over estimate of the CO_2 dissolved in brine. A mesh sensitivity analysis will be carried out in the near future. The model with smaller vertical extension has a number of cells equal to 115668, while the mesh used to include an additional portion of caprock (Fig 1.b,c) is identical to the previous one, but three additional cell layers have been added, increasing the number of cells to 123930. PFLOTRAN discretises the flow and transport equations using a fully implicit finite volume method that can be considered first order in time and space [1]. The software uses an adaptive time step scheme to accelerate the simulation, increasing and decreasing the time step based on the convergence speed. Even if the mesh of the present model is structured, featuring some distorted hexahedron cells, the discretisation has been considered unstructured when loaded in PFLOTRAN. This was done to validate the software performance and its automatic domain decomposition algorithm when unstructured grids are adopted. All the simulations have been performed using a four core machine (Intel(R) Core(TM)2 Quad CPU Q9550 @ 2.83GHz), with Ubuntu 12.01 as the operating system.

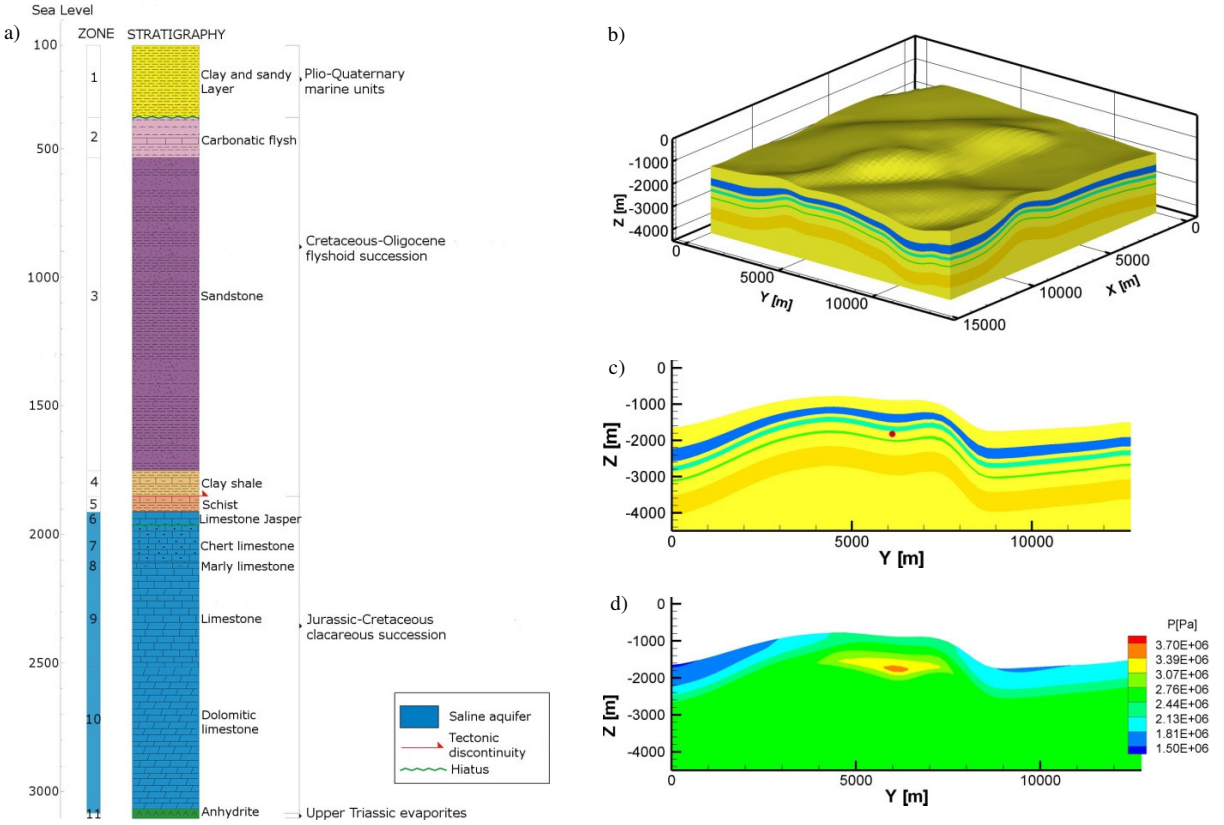

Fig.1 – Geological model: a) simplified stratigraphy on a cross section of the injection well; b) 3D model with a reduced caprock portion including the following layers (L): 300 m portion of L3 + L4 + L5; c) vertical cross section of the geological layers at x=7125 m. d) Overpressure contours in the vertical cross section at x=7125 m computed as the difference between the pressure at the end of the injection and the initial unperturbed pressure, case with larger caprock.

3.1. Multiphase flow model: long- term prediction of the injected CO_2

The Span and Wagner equation of state (EOS) [3] is used to compute the SC-CO_2 properties, while the Duan EOS [5] is employed for the resulting mixture derived from the dissolution of SC-CO_2 in brine. The fluid properties of SC-CO_2 that contain dissolved brine are taken to be identical to those of the pure SC-CO_2 due to the typically low concentrations of brine. Since no core sample measurements were available for either the caprock or the reservoir, linear capillarity pressure and relative permeability functions have been adopted, assuming a zero critical capillarity pressure to consider a worst-case scenario for CO_2 leakages. Under this assumption the CO_2 flow through the caprock is impeded only by the low permeability value. The brine and gas residual saturations are taken equal to 0.1 and 0.05 respectively, and a maximum capillarity pressure of 10^6 Pa has been imposed when the water saturation approaches a zero value. The same functions and parameters have been used for each of the 9 geological layers considered. The diffusivity coefficient within the liquid phase (e.g. diffusion of CO_2 in brine) was computed according to [5] from the viscosity of the fluids at reservoir temperature and set at 4.04×10^{-9} m^2/s. The diffusion coefficient within the gas phase depends on pressure and temperature, and it is computed with the formula proposed by [12] using a diffusion coefficient at reference condition (T=273.15 K, p= 1 atm) equal to 2.13×10^{-5} m^2/s.

Table 1 – Petrophysical and thermal properties of the materials used in the 9 geological layers included in the model from the top to the bottom.

Geological Layer	Density (kg/m^3)	Heat Capacity (J/kg °C)	Initial Permeability (m^2)	Initial Porosity
Caprock 1	2500	1137	7.65×10^{-18}	0.03
Caprock 2	2600	1170	7.65×10^{-18}	0.03
Caprock 3	2600	870	2.04×10^{-17}	0.05
Caprock 4	2600	900	2.04×10^{-17}	0.05
Reservoir 5	2600	920	2.04×10^{-14}	0.10
Reservoir 6	2600	940	1.04×10^{-14}	0.10
Reservoir 7	2600	940	2.48×10^{-14}	0.10
Reservoir 8	2600	940	2.48×10^{-14}	0.1
Reservoir 9	2800	1870	1.84×10^{-16}	0.06

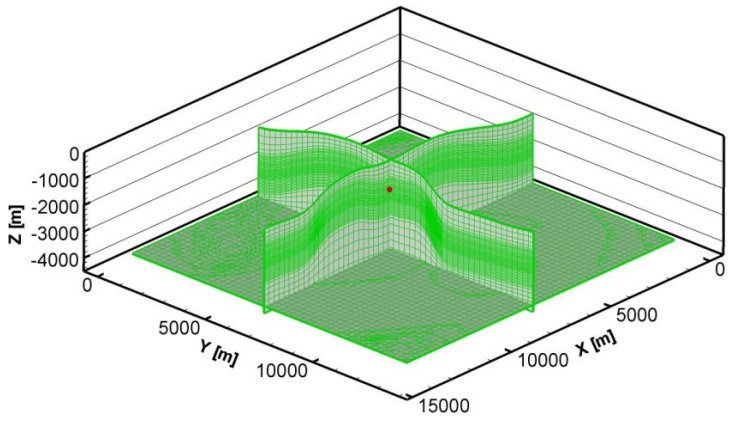

Fig. 2 –3D computational mesh for the vertical extension option of Fig 1.b, the red dot indicates the injection well.

Before the injection, the reservoir is assumed to be fully saturated in brine with a constant concentration of NaCl (0.4 M – 24 g/L). The pressure is assumed to be hydrostatic, and an initial temperature is computed from the known thermal gradient (3.28 °C/100 m) and the given temperature at the seabed (17 °C). In the multiphase flow

model the salt concentration is kept constant throughout the simulation, and its value is used to compute the properties of the CO_2/brine mixture. Due to the pressure and temperature ranges found in the reservoir, significant salt precipitations and change in salinity are not expected, and this assumption can be considered to be valid in first approximation, at least for the multiphase flow solution. In the reactive transport model the ions Na^+ and Cl^- are transported and have varying concentration in space and time (see section 3.2). To reflect the model domain vicinity to the normal faults that delimit horizontally the reservoir, closed (no flux) boundary conditions have been imposed at the side boundaries, with no flux boundary conditions at the top and bottom surfaces that delimit the vertical extension of the model. The two-component, two-phase flow is modelled using a flash method [9], in which the solution variables are the pressure, the total component mole fraction for CO_2, and the temperature. The first two variables are associated with the solution of mass balance equations, while the temperature is obtained by solving the energy equation, [1]. The flash method permits the solution for the same set of variables regardless of phase composition, (only brine, brine/CO_2, only CO_2). Theoretically, it is more robust than the alternative variable switch approach, and in some cases it can reduce the computational time thanks to the use of larger time steps. The flow simulation is carried out up to 2000 years to evaluate dissolution of CO_2 in the formation waters and eventual leakages into the caprock, limiting the maximum time step size to 50 days.

Fig 3 shows the CO_2 plume extension and the molar concentration of CO_2 in brine at the end of the injection period (20 years). Figure 4 shows the CO_2 plume development and the corresponding distribution of the molar concentration of CO_2 in brine over time in a vertical plane crossing the injection cell. During the injection, the CO_2 tends to migrate upwards where it is trapped by the caprock. As a consequence the plume spreads horizontally following the caprock topography. The over pressure in the well, at the end of the injection period, is ~38 bars, and the CO_2 plume covers a ~3.5 km diameter area (3.75 km in the x direction and 3.5 km in the y direction). The over pressure reaches high values everywhere in the reservoir (see Fig. 1.d) because closed side boundaries have been imposed, while a low permeability layer is found at the bottom. The reservoir acts as a closed domain pressurised by the CO_2 injection, with the leakages through the caprock and the CO_2 dissolution in brine being the only two phenomena able to ease the pressure. After 200 years the maximum overpressure is ~28 bars, and it is still ~22 bars at the end of the simulation (2000 years). This model facilitates the CO_2 dissolution in brine and tends to overestimate the pressure build up in the far field, so the values computed for both these parameters can be seen as upper limits. When the injection is stopped, the CO_2 saturation decreases and the concentration of CO_2 in brine increases due to the dissolution of CO_2 in brine (solubility trapping). The CO_2-enriched brine is heavier than the underlying fluid, and it starts moving downwards, generating finger-like shapes at high CO_2 concentration, creating counter flows of fresh brine. The prediction of these fingering phenomena requires a much higher grid resolution than the one employed in this model, a resolution which is impractical for the large scales involved when building a reservoir model. The downwards density driven flow, shown in Fig. 4, is strongly dependent on the grid resolution, which becomes the major controlling parameter. The elaboration of a sub-scale model to take account of fingering and compute a corrected downwards flux is a hot topic within the research community, [10].

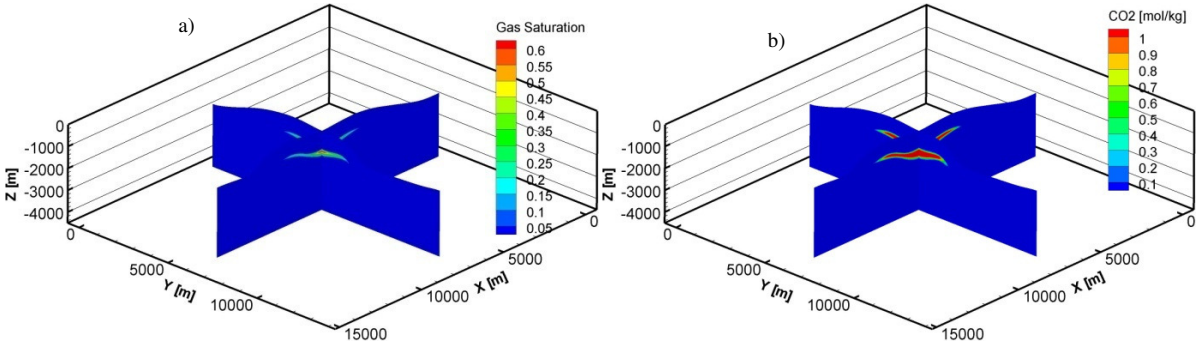

Fig. 3 – Contour plots of SC-CO_2 saturation (a), and molar concentration of CO_2 in brine (b), in two vertical planes crossing the injection cell (x=7125 m, y=6125 m).

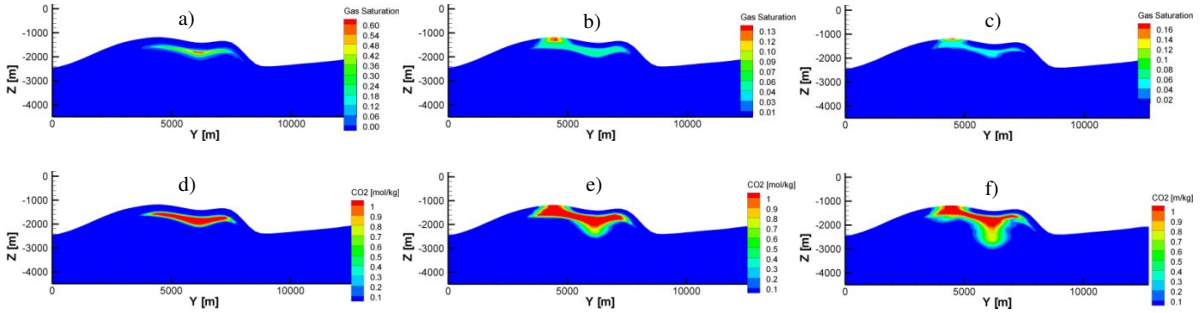

Fig. 4 Contour plots in a vertical plane crossing the injection cell (x=7125 m). CO_2 saturation at 20 y (a), 1000 y (b), 2000 y (c). Molar CO_2 concentration in brine at 20 y (d), 1000 y (e), 2000 y (f)

A minor SC-CO_2 flow into the caprock is observed (Fig. 4.b-c) in the long-term prediction (1000 y and 2000 y). The SC-CO_2 is dissolving very slowly in brine, and a small amount, not yet dissolved, has the time to penetrate the caprock. The overpressure in the plume remains considerably high for many years after the injection, while the buoyancy forces keep the SC-CO_2 in contact with the caprock. Under this overpressure, the SC-CO_2 starts flowing slowly through the caprock, facilitated also by the assumption of a zero critical capillarity pressure. The observation of these leakages suggests to rebuild a model with a vertical extended caprock to remove the artificial no flux condition and to study the development of the infiltration, but also to estimate and assess some more realistic non-zero critical capillarity pressure values. Fig 4.b,c show the zone of SC-CO_2 residual trapping: this is the blue shaded area that has been invested by the SC-CO_2 plume during the injection, which has undergone a brine rewetting after the injection was stopped. The hysteresis effects are not taken into account, however a residual gas saturation equal to 0.05 is used for the SC-CO_2 relative permeability function.

After 1000 years 69% of the SC-CO_2 injected is dissolved in brine, 9% is trapped in the hosting matrix pores; after 2000 years the dissolution reaches 79%, while the residual trapping reduces to 6% because some of the trapped SC-CO_2 has dissolved into the fresher brine drawn in by density driven flows.

In the simulations described above, the computational domain that includes the smaller portion of caprock has been used (L4 + L5), Fig. 1.a. The effect of the caprock extension on the far-field overpressure has been assessed running again the multiphase flow simulation adding a portion of caprock (~300 m of the layer 3). No significant differences are found in the maximum overpressure computed in the domain at the end of the injection. However, for the case with the thinner caprock, the model predicts overpressures up to 3 bars larger in the domain vertical boundaries. Fig. 1.d shows the overpressure field for the case with extended caprock. As discussed in [8], the brine and the SC-CO_2 flow through the caprock can ease the overpressure in the far field: the more imperfect the caprock, the more it will impact on the far-field overpressure; and since the caprock in this case has a permeability of the order of 10^{-17} m^2, a domain that extends for a few km is enough to observe such effects.

3.2. Geochemical model: effects of the mineral dissolution/precipitation

A campaign of reactive transport simulations to study the effect of mineral/dissolution precipitation in the reservoir and in the caprock is currently ongoing for the model presented in this work. The reservoir consists of porous limestone (mainly calcite) and marly limestone deposits with a significant component of carbonate (see Table 3, calcite and dolomite ranging from 66% to 99% by vol.) and minor clay minerals (illite, chlorite and Ca-montmorillonite). The caprock includes allochtonous marly calcarenites and clay marls, made up of about 70% by vol. of carbonates and 30% by vol. of silicate minerals, represented by quartz and clay minerals, Table 3. A system of multi-component reactive transport equations is solved at the end of each flow time step, [1]. The aqueous species are considered to be in equilibrium, and the corresponding laws of mass action are used to express a set of (secondary) species with respect to a set of (primary) species, for which the transport equations are solved (i.e. the

transported quantities are the total concentration of the primary species). Table 2 lists the aqueous species included in the reactive transport model.

Table 2: list of primary and secondary species considered in the geochemical model.

Primary species	Secondary species
H+, $CO_{2(aq)}$, Na^{+}, K^{+}, Fe^{+2}, Mg^{+2}, Al^{+3}, Cl^{-}, Ca^{+2}, SO_4^{-2}, $SiO_{2(aq)}$	OH^{-}, HCO_3^{-}, CO_3^{-}, $CaCO^3_{(aq)}$, $CaOH^{+}$, $NaOH_{(aq)}$, $NaCO_3^{-}$, $NaHCO_{3(aq)}$, $CaHCO_3^{+}$, $Mg\,HCO_3^{+}$, $MgCO_{3(aq)}$, $MgOH^{+}$, $H3SiO_4^{-}$, $Al(OH)_2^{+}$, AlO_2^{-}, $HAlO_{2(aq)}$, $NaAlO_{2(aq)}$, $Al(OH)_{3(aq)}$, $AlOH^{+2}$, $CaCl^{+}$, $CaCl_{2(aq)}$, $MgCl^{+}$, $NaCl_{(aq)}$, $NaHSiO_{3(aq)}$, $HSiO_3^{-}$, $FeCl^{+}$, $FeHCO_3^{+}$, $FeCO_{3(aq)}$, $FeCl_4^{-2}$, $CaSO_{4(aq)}$, HSO_4^{-}, $Al(SO4)_2^{-}$, $AlSO_4^{+}$, $FeSO_{4(aq)}$, $KHSO_{4(aq)}$, $MgSO_{4(aq)}$, $NaSO_4^{-}$

Table 3: Mineral species volume fraction (% by volume) and mineral surface areas (cm2/cm3) for each geological layer.

	Caprock				Reservoir										Bottom	
	Layer 2		Layer 3		Layer 4		Layer 5		Layer 6		Layer 7		Layer 8		Layer 9	
	Vol.	A_0	Vol.	A_0	Vol.	A_0	Vol.	A_0	Vol.	A_0	Vol.	A_0	Vol.	A_0	Vol.	A_0
Calcite	83.7	1500	61.0	1500	95.3	1200	66.1	4615	96.0	2000	99.3	2000	74.7	3000	0.8	250
Quartz	5.4	337	36.0	1814	3.3	752	31.4	600	3.7	88	0.6	89	0.6	545	-	-
Dol.-Dis	-	-	-	-	-	-	-	-	-	-	-	-	24.0	4573	0.2	248
Illite	3.5	750	1.2	625	1.2	3000	0.2	3000	-	-	-	-	-	-	-	-
Chlorite	3.2	750	0.2	625	-	-	0.2	3000	-	-	-	-	-	-	-	-
Ca-Montm	4.1	1000	1.5	625	-	-	2.0	3000	0.2	1000	-	-	0.6	2000	-	-
Anydrite	-	-	-	-	-	-	-	-	-	-	-	-	-	-	98.9	276
Kaolinite	-	-	-	-	-	-	-	-	-	-	-	-	-	-	-	-
Dawosonite	-	-	-	-	-	-	-	-	-	-	-	-	-	-	-	-
Chalcedony	-	-	-	-	-	-	-	-	-	-	-	-	-	-	-	-
Phlogopite	-	-	-	-	-	-	-	-	-	-	-	-	-	-	-	-

The mineral dissolution/precipitation reactions are considered kinetic, and modelled with a transition state theory formulation, [1]:

$$r = A\left[k_{0-a} \exp\left(-t_f E_{a-a} / R\right) a_{H^+}^{n_1} + k_{0-n} \exp\left(-t_f E_{a-n} / R\right) + k_{0-b} \exp\left(-t_f E_{a-b} / R\right) a_{OH^-}^{n_3} \right]$$
$$t_f = \left(1/T - 1/298.15\right) \quad (1)$$

where A is the specific mineral surface area, E_a is the activation energy, k_0 is the rate constant at 298.15 K, R is the gas constant, T the absolute temperature in Kelvin. Additional terms were added to or removed from Eq. (1) to account for other mechanisms, i.e. as those catalysed by HCO_3^{-}, see Table 4. All the kinetics parameters used in Eq. (1) are from [11] and listed in Table 4. Specific reactive surfaces of mineral are relatively difficult to be measured, especially for multi-mineral systems, since only part of the mineral surface participates in the reactions (e.g. [12]). During kinetic reactions, the specific surface area increases or decreases as the morphology of the mineral changes [13]. In this study the initial reactive surface area of each mineral (Table 3) was calculated as a geometric surface area of spheres on the basis Scanning Electronic Microscopy analysis on rock samples outcropping inland [2]. For clay mineral a plate-like grain was considered (e.g. [14]). To account for the discrepancy between the BET surface area and the geometric area (surface roughness; e.g. [15]), and for the

interaction fluid-mineral occurring only in selective sites, [15], the reactive surface areas used in numerical simulations are decreased by one order of magnitude, see Table 3.

Table 4 -mineral kinetic parameters

	K298.15 (mol×m^{-2}×sec^{-1})			Ea (kJ× mol^{-1})				
	acid	Neutral	base	acid	Neutral	Base	n_1	n_3
Calcite	5.0×10^{-1}	1.6×10^{-6}	6.3×10^{-22}	51.7	38.0	-	0.5	0.823
Quartz	-	5.9×10^{-13}	-	-	74.5	-	-	-
Dolomite-Dis	6.5×10^{-4}	3.0×10^{-8}	7.8×10^{-6}	36.1	52.2	34.8	0.5	0.5
Illite	1.1×10^{-11}	1.6×10^{-13}	3.0×10^{-17}	32.6	35.0	58.9	0.34	0.40
Kaolinite	4.9×10^{-12}	6.9×10^{-14}	8.9×10^{-18}	65.9	22.2	17.9	0.77	0.472
Chlorite	7.8×10^{-12}	3.0×10^{-13}	-	88.0	88.0	-	0.5	-
Ca-Montm	2.0×10^{-13}	3.9×10^{-15}	3.9×10^{-15}	48.0	48.0	48.0	0.2	0.13
Anydrite	-	6.5×10^{-4}	-	-	14.3	-	-	-
Secondary minerals								
Dawosonite	-	1.3×10^{-9}	-	-	62.8	-	-	-
Chalcedony	-	5.9×10^{-13}	-	-	74.5	-	-	-
Phlogopite	-	4.0×10^{-13}	-	-	29.0	-	-	-

Precipitation of potential secondary minerals is represented with the same kinetic expression as for the dissolution. Since kinetic parameters for precipitation rates are available for few minerals, only parameters for the neutral mechanism are used to describe precipitation. For the secondary minerals, an initial surface reactive area equivalent to a sphere of radius equal to 10^{-6} m, and a small volume fraction of 10^{-6} was assigned (Table 4). The equilibrium constants for the aqueous species and minerals used in this study are taken from EQ3/6 V7,2 database [16] and recalculated at an average reservoir pressure of 204 bars using SUPCRT [17].

The initial concentration of the primary species is computed by performing a pre-injection simulation to create an initial water in equilibrium with the primary minerals included. The brine that is left to react with minerals is imposed the prescribed concentration of salt, and a concentration of dissolved CO_2 such as the pH measured in the reservoir is matched. Due to the fast kinetic of carbonate minerals and the high reactive surface area, a time span of 20 years is enough to reach the equilibrium. Zero gradient conditions are applied to all the species transported in all the domain boundaries, and the diffusion coefficient for the aqueous phase is taken equal to the one used in the multiphase flow simulation (see section 3.1). The dispersivity effects are not considered.

The coupling between the flow and the reactive transport occurs in two ways. The CO_2 pressure and the temperature computed in the flow module are imposed to the chemical speciation in the reactive transport, and the mineral reaction computed in the reactive transport updates the porosity and permeability used in the next flow time step computation. The porosity is updated accounting directly for the variation of the mineral volume fractions, while the permeability changes can be computed relating the permeability to the porosity. Since the work on the reactive transport is still ongoing, and particular attention is being given to the analysis of mineral dissolution/precipitation processes and to their activation factors, the changes in permeability are not included at present. Once a good degree of confidence is achieved with the mineral kinetic reactions that are occurring in the long-term, then their effects in permeability changes will be assessed. The specific mineral surface areas are updated at each time step with the following formula, where A_0 is the initial value of the mineral surface area:

$$\mathrm{A} = A_0 \left(\varphi/\varphi_0\right)^{2/3} \tag{2}$$

After the generation of the initial conditions, the CO_2 injection starts to perturb the geochemical system, and the model is run up to a physical time of 1000 years imposing an initial time step of a few seconds limiting the maximum time step to 50 days. The simulation took 2 days and 22 hours using the computer described in section 3. Figs. 5.a and 5.b show the brine acidification and the porosity changes at the end of the injection period (20 years). The pH drops to a value of ~4.7 causing a small but noticeable dissolution of calcite, quartz, chlorite and illite. The porosity changes are very small, of the order 0.1-0.5%. A small increase in porosity is observed in the injection region and the zone just above it, while moving away from the well a small decrease is found in a circular area surrounding the injector. This is explained by the precipitation of Montmorillonite (see Fig 5.d), which precipitates where it finds a water reach in calcium (Ca^{+2}), magnesium (Mg^{+2}) coming from the dissolution of chlorite (see Fig. 5.e) and aluminium (Al^{+3}) due to the dissolution of illite (see Fig. 5.f).

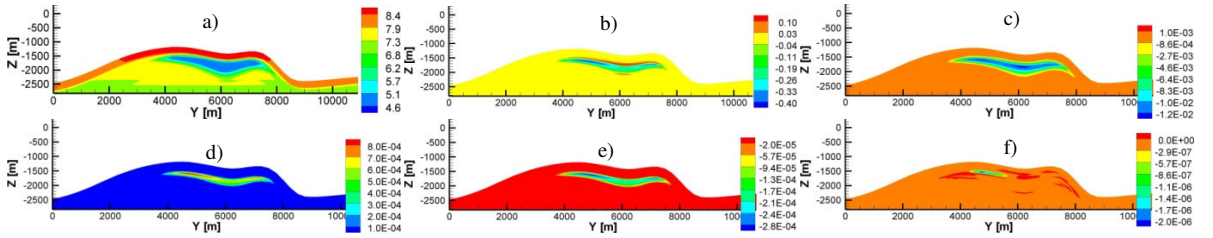

Fig. 5 – Geochemical analysis at the end of the injection (20 years) in the region surrounding the injection point, in the vertical plane at x=7125 m. a) pH; b) porosity change %; c) calcite v_f change %; d) Montmorillonite v_f change; e) Chlorite v_f change; f) Illite v_f change. The porosity and the volume fraction (v_f) changes have been computed as differences between the value at the end and before the injection.

After 1000 years from the beginning of the simulation, the change of porosity are more remarkable (~ 5%), Fig 6.b. The pH in the area surrounding the well increases due to the less acid brine drawn in by the density driven flow of the CO_2 enriched brine, see Fig 6.a. The calcite is the main mineral responsible for the porosity change, Fig. 6.c, however other minerals such as the quartz, the chlorite, the illite and the montmorillonite still have a contribution to the final porosity value. An observable dolomite dissolution is also recorded in the lower end of the pH plume while a considerable calcite precipitation (~4%) and consequent porosity reduction can be noticed in the infiltration area. This could enhance the sealing properties of the caprock, and to assess in what measure, it would be useful to run the same model with an extended caprock and introducing the permeability changes.

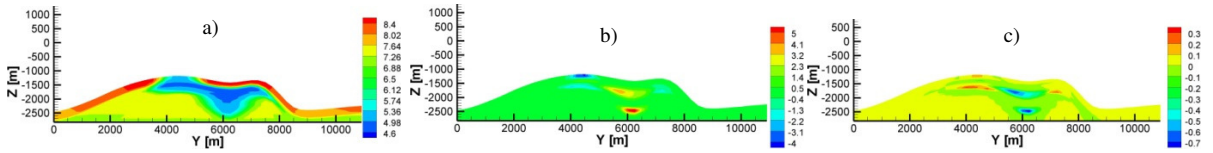

Fig. 6 - Geochemical analysis at 1000 years in the region surrounding injection point, in the vertical plane at x=7125 m. a) pH; b) porosity change %; c) calcite v_f change %. The changes have been computed as differences between the values at 1000 y and before the injection.

No relevant precipitations have been observed for the secondary minerals included in the model, only a small precipitation of kaolinite. In addition, a larger dissolution of calcite was expected. The abundance of Fe^{2+} due to chlorite dissolution encouraged the authors to add additional secondary carbonate minerals that might also precipitate such as the siderite and ankerite, which could favour the mineral trapping of the CO_2 injected.

4. Conclusion

In the work presented, PFLOTRAN has been used to model a potential CO_2 storage site located offshore the west coast of Italy. The model gave an estimate of the CO_2 plume extension (~3,5 km diameter for an injection of 30 Mtons of CO_2 over 20 years) and predicted a maximum pressure build up of ~38 bars at the end of the injection

operations. The solubility trapping has been quantified computing a dissolution in brine of 69% and 79% of the total amount of CO_2 injected after 1000 years and 2000 years respectively. The residual trapping has also been found to play an important role, with a percentage of the injected CO_2 locked into the hosting matrix pores equal to 9% and 6% after 1000 and 2000 years respectively. Minor CO_2 leakages through the caprock have been identified in the shallowest part of the reservoir assuming a zero critical capillarity pressure to consider the worst-case scenario. The large and lasting overpressure in the reservoir caused the leakages to reach the top domain boundary. Finally, some preliminary simulation being done as part of an ongoing effort to couple a geochemical model to the multiphase flow simulations reveals small changes in mineral volume fraction and porosity (~5% after 1000 years). The work carried out so far highlights the necessity to increase the vertical extension of the model to include a larger portion of the caprock in order to assess the fate of the CO_2 leakages observed. The early geochemical model results suggest testing other secondary minerals that could precipitate and benefit the mineral trapping (still not quantified), and to assess the effect of permeability changes on the multiphase flow solution. The authors are also working on a mesh sensitivity analysis and the comparison/validation of PFLOTRAN against TOUGHREACT.

References

[1]Hammond, G.E., Lichtner, P.C., Lu, C. and Mills, R.T. PFLOTRAN: Reactive Flow & Transport Code for Use on Laptops to Leadership-Class Supercomputers. *Groundwater Reactive Transport Models*, 2012, 142-160.

[2] Montegrossi, G., Cantucci B., Vaselli O., Quattrocchi F. Reconstruction of porosity profile in an off-shore well. *Bollettino di Geofisica Teorica ed Applicata*, 2008, 49 (2), 408-410.

[3] Span, R., Wagner, W. A New Equation of State for Carbon Dioxide Covering the Fluid Region from the Triple-Point Temperature to 1100 K at Pressures up to 800 MPa, *J. Phys. Chem. Ref. Data*, 1996, 25, 6, 1509–1596.

[4] Duan, Z., Hu, J., Li, D., and Mao, S. *Densities of the CO2-H2O and CO2-H2O-NaCl Systems up to 647 K and 100 MPa, Energy & Fuels*, 2008, 22, 1666–1674.

[5] Tamimi, A., Rinker, E. B., and Sandall, O.C. Diffusion Coefficient for Hydrogen Sulfide, Carbon Dioxide, and Nitrous Oxide in Water over the Temperature Range 293-368 K. *J. Chem. Eng. Data*, 1994, 39(2), 330-332.

[6] Vargaftik, N.B. *Tables on the Thermophysical Properties of Liquids and Gases*, 2nd Ed., New York, NY, John Wiley & Sons, 1975.

[7] Walker, W.R., Sabey, J.D., and Hampton, D.R. *Studies of Heat Transfer and Water Migration in Soils, Final Report*. Department of Agricultural and Chemical Engineering, Colorado State University, Fort Collins, CO, 80523, 1981.

[8] Birkholzer, J.T., Zhou, Q., Tsang, C.F. Large-scale impact of CO2 storage in deep saline aquifers: A sensitivity study on pressure response in stratified systems. *International Journal of Greenhouse Gas Control*, 2009, 3(2),181-194.

[9] Michelsen, M. L. The isothermal flash problem. Part 1. Stability. *Fluid Phase Equilibria*, 1982, 9, 1–19.

[10] MacMinn, C. W., Neufeld, J. A., Hesse, M. A., & Huppert, H. E. Spreading and convective dissolution of carbon dioxide in vertically confined, horizontal aquifers. *Water Resources Research*. 2012, 48(11)

[11] Palandri, J.L., and Kharaka, Y.K, 2004. A compilation of rate parameters of water-mineral interaction kinetics for application to geochemical modelling. *U.S. Geological Survey Water-Resources Investigations Report 04-1068*.

[12] Xu,T., Sonnenthal,E., Spycher, N., Pruess,K. TOUGHREACT:A simulation program for non-isothermal multiphase reactive geochemical transport in variably saturated geologic media: Applications to geothermal injectivity and CO2 geological sequestration. *Computers & Geosciences*,2006, 32(2), 145-165.

[13] Wilson, M.J. Chemical weathering of some primary rock-forming minerals. *Soil Sci*. 1975, 119, 349-355.

[14] Marini, L. Geological sequestration of carbon dioxide: Thermodynamics, kinetics, and reaction path modelling. *Developments in Geochemistry*, 2007, 11, 453

[15] Zerai, B., Saylor, B.Z., and Matisoff, G. Computer simulation of CO2 trapped through mineral precipitation in the Rose Run Sandstone, Ohio. *Applied Geochemistry*, 2006, 21, 223–240.

[16] Wolery, T.J. EQ3/6: Software package for geochemical modeling of aqueous systems: package overview and installationguide (version 7.2). *Lawrence Livermore National Laboratory Report UCRL-MA-10662 PT I*, Livermore, California, 1992

[17] Johnson, J. W., Oelkers, E. H. and Helgeson, H. C. SUPCRT92: a software package for calculating the standard molal thermodynamic properties of minerals, gases, aqueous species, and reactions from 1 to 5000 bars and 0° to 1000°C. *Laboratory of Theoretical Geochemistry*, University of California, Berkeley, 1992.